Int J Adv Manuf Technol (2014) 70:1673–1681
DOI 10.1007/s00170-013-5441-8

ORIGINAL ARTICLE

A new current hybrid inertia friction welding for nickel-based superalloy K418–alloy steel 42CrMo dissimilar metals

Jian Luo · Longfei Li · Yaling Dong · Xiaoling Xu

Received: 16 April 2013 / Accepted: 15 October 2013 / Published online: 30 October 2013

Abstract The nickel-based superalloy K418 and alloy steel 42CrMo dissimilar metals friction welding joints lack strength and toughness due to high hardening and poor joining quality at the friction interface. To resolve this issue, a new current inertia friction welding (CIFW) method is carried out by hybrid an external additional electronic current in inertia friction welding (IFW) process. The characteristics of welding formation, the elements' diffusion, and the mechanical properties of K418–42CrMo dissimilar metal joints are studied by scanning electron microscope, energy dispersive spectrometer, and X-ray diffractometer tools. The experimental results show that hybrid additional electronic current has a significant positive influence on interface characteristics of IFW joints. The required welding time for CIFW to complete a good qualified joint is shortened due to mixture actions of both friction heat and resistance heat. The width of the element diffusion zone increases in CIFW joints, and elements in 42CrMo side diffuse through the K418/42CrMo interface into the K418 side in CIFW joints. The width of the K418/42CrMo bonding interface increases in CIFW joints. The microhardness at the K418/42CrMo bonding interface is decreased in CIFW joints. The mechanical tensile property of CIFW joints is increased obviously. The interface bonding pattern becomes jagged and interlocking perfect formations. These above changes improve the joining quality of K418–42CrMo dissimilar metal friction welding joints. The heat treatment effect and resistance heat effect originated from hybrid external electronic currents are discussed by comparing CIFW with IFW. A new model is proposed to illustrate the interface's evolution and development mechanism in K418–42CrMo dissimilar metal CIFW.

Keywords Inertia friction welding · Current hybrid · Dissimilar metals · Microstructure · Interface feature

J. Luo (✉) · L. Li · Y. Dong
State Key Lab of Mechanical Transmission, Chongqing University, Chongqing 400030, China
e-mail: luojian2007@gmail.com

X. Xu
Chongqing Honglingxiang Mechanical Development Co. Ltd, Chongqing 400030, China

1 Introduction

The friction welding has been widely employed in traditional industrial fields, such as automotive, tool manufacturing, and petrochemical industries, because of their unique advantages including good properties, high efficiency, low cost, and joint reliability. It has found promises for joining in high-tech areas such as aerospace, nuclear energy, and deep-ocean development [1–3].

Joining of dissimilar metals is one of the most essential needs from industries. Friction welding has been successfully used to join dissimilar metals in many fields. Meshram et al. [4] investigated dissimilar metal combinations of Fe, Cu, Ti, and Ni; results showed that a rise in the interaction time can reduce the strength in eutectoid forming and insoluble systems but increase the strength in soluble systems. Huang et al. [5] studied the nickel-based superalloys 720Li and IN718 inertia friction welding joints and pointed out that the different high temperature mechanical properties of the two different kinds of alloys can cause a difference in the width of the heat affected zone. Sare and Ismail [6] and Moat et al. [7] studied dissimilar steels friction welding joints, and detected that the tensile strength of the welding specimens is very close to that of base materials. Luo et al. [8], Sahin [9], and Kimura et al. [10] investigated mechanical and metallurgical properties of austenitic stainless steel–copper alloy friction welding joints. Friction welding of similar and dissimilar bulk glassy alloys was also explored [11–13]. At the same time, some friction

welding joints with different dissimilar materials were also studied, including steel–Al alloy [14–17], steel–titanium [18], steel–nickel alloy [19], steel–ceramic [20], steel–Cu alloy [21], and Al alloy–Cu alloy [22].

Engine turbocharger rotor is an important welding structure that requires joining Ni-based cast superalloy K418 to quench-tempered alloy steel 42CrMo. This is a typical dissimilar material welding. It is difficult owing to the significant difference in chemical composition and mechanical properties of these two materials. Laser or electronic beam is suitable for this application, but its high costs affect its competitiveness [23]. On the other hand, the friction welding is one of the most used engineering applications in K418–42CrMo dissimilar materials joining [24, 25].

In dissimilar metal friction welding, it is necessary that many elements diffuse each other from both sides of the joint interface. It is easy to produce some brittle intermetallic compounds owing to transfer or scatter of dissimilar metal elements on the friction contact surface. The brittle intermetallic compounds are frequently found in the binding region because of the elements diffusion and interaction with each other. It is harmful to the bonding performance of dissimilar metal joints [25, 26]. Du et al. [27] shows that "Hard" technical specification of friction welding can control the interface heat or element transfer process in K418–42CrMo dissimilar metal joints, helping decrease the heat transfer and element scatter action and thus prevent the carbide compound band from forming on the friction contact surface. The nickel-based superalloy K418–alloy steel 42CrMo dissimilar metal friction welding joint lacks the strength and toughness; one of the reasons is due to the high hardening of the friction interface affecting the joining quality [24–28].

Current inertia friction welding (CIFW) is a hybrid method with properties of both friction welding and resistance welding process. Applied current provides resistance heat to heat the friction interface, helping to improve the weld quality [29–31]. This study aims to understand the external current's effect, to control the brittle intermetallic formation on the interface, and to improve the bonding reliability. In this paper, traditional inertia friction welding (IFW) and CIFW experiments and tests are carried out for K418–42CrMo dissimilar metal joints. The influence of hybrid additional current on the friction welding process, weld formation, metallurgical characteristics, and mechanical performances of these joints will be studied.

2 Experimental procedures

2.1 Materials

The materials used in this work are Ni-based casting superalloy K418 and the quench-tempered alloy steel 42CrMo (ASTM 4140, DIN 42CrMo4). The thermal–physical properties are shown in Table 1, and the chemical compositions (wt%) of K418 and 42CrMo are listed in Tables 2 and 3, respectively.

2.2 Welding procedure

Figure 1 shows the welding specimen structure and a CIFW technical diagram. The diameter of the clamping parts is 60 mm in order to hold workpieces. The workpiece are columns with 8 mm in diameter and 10 mm in length. The friction contact surface is cleaned using acetone and then dried before welding. CT-25 type multipurpose friction welding equipment is used. Its specifications include rotating speed of 0–5,000 rpm (stepless adjust to enable), the maximum axial pressure of 250 kN, and maximum working travel distance of 1,500 mm (welding workpiece length enable). The working program or process is automatically operated by a microcomputer monitoring and controlling system.

In CIFW, the 42CrMo workpiece is not a rotating part, while the K418 workpiece is. When the rotating flywheel is up to the predetermined speed, it detaches from the drive motor. The 42CrMo workpiece will contact the K418 workpiece quickly with a hydraulic driving force. At the same time, the external additional electronic current passes through the interface. The total welding heat at the interface of the two parts includes the resistance heat and friction heat transformed from the kinetic energy in the rotating flywheel. In this way, the interface is heated to a suitable welding temperature for welding, the forge pressure make a tight bonding joint with a flash formation, and the oxide and other impurities are ejected from the friction interface. Surface activation, element diffusion, and grain recrystallization occur in the bonding region. The additional current is turned off when the flywheel stops or the friction welding process finishes.

In our experiments, the predetermined speed of the flywheel is 3,000 rpm. The welding parameters of the conventional inertia friction welding are as follows: moment of inertia, 0.636 kg m^2; friction pressure, 42 MPa; forge pressure, 78 MPa; and maximal welding time, 3 s. In CIFW, the preset welding parameters of inertia moment, friction pressure, forge pressure, and welding time are the same as those for the conventional inertia friction welding except that a current density of 5.1 A/mm^2 was applied. The same preset

Table 1 Thermal–physical properties of K418 and 42CrMo

Materials	Density (kg/m^3)	Melting point (°C)	Elasticity modulus (GPa)	Specific heat capacity (J/kg °C)	Coefficient of heat conductivity (W/m°C)
K418	8,000	1,295	144	529	9
42CrMo	7,850	1,390	165	470	39

Table 2 The composition of Ni-based casting superalloy K418 (wt%)

C	Cr	Mo	Nb	Al	Ti	Zr	B	Mn	Si	P	S	Fe	Ni
0.08–0.16	11.5–13.5	3.8–4.8	1.8–2.5	5.5–6.4	0.5–1.0	0.06–0.15	0.008–0. 020	0.50	≤0.50	≤0.015	≤0.010	≤1.0	Balance

welding parameters will provide a comparable benchmark between IFW and CIFW. In fact, the quality control method of the welding procedure in this paper is plastic deformation of the welding joints, and the plastic deformation comes from the friction heating and axial pressure. When the plastic deformation of the welding joints is enough, the welding procedure is finished despite the preset welding time. Axial shortening of welding joints is one of the practical quality controlling parameters, which is measured by the displacement transducer in the friction welding machine. The actual welding time between IFW and CIFW may thus be different. The welding parameters and its optimization for K418–42CrMo dissimilar metals have been achieved on our previous research works for conventional IFW.

2.3 Measurement and observation methods

The electrospark wire-electrode cutting method is used to cross-section the joint on the axial direction. The longitudinal sections are prepared for microstructure observations by mechanical polishing and chemical etching techniques with a standard metallographic procedure. For dissimilar metal joints, the K418 side is etched by aqua regia, while the 42CrMo side is etched by an alcohol solution with 4 % nitric acid.

The samples are KQ-100E ultrasonic cleaner washed before they are examined by a TESCAN VegaII LMUSEM scanning electron microscope (SEM) for the microstructure characteristics. Element distributions are analyzed using an OXFORD ISIS300 energy dispersive spectrometer, which is a tool attached to the SEM. The Rigaku D/max-2500 PC X-ray diffractometer (XRD) is used to study the phase composition with a CuKα radiation at 40 kV/150 mA. A MC010-HV-1000 micro-Vickers is used for microhardness testing; the load is 9.8 N, and the duration for loading is 10 s. The RGM2100 electronic universal testing machine is used for mechanical tensile testing. There are two National Standards of the People's Republic of China (GB2649-89 methods of sampling for mechanical properties test of welded joint and GB/T 2651-2008 tensile test methods on welded joint) to be obeyed in this paper.

3 Experimental results

3.1 Welding joint

Figure 2 shows the macrostructure of the welding joints from conventional IFW and CIFW, respectively. No defects, such as inclusions and porosity, are found which may be seen in certain fusion welding methods. There are two differences in the bonding formation between IFW and CIFW. Because the 42CrMo base material is softer than the K418 base material, the welding flash forms on the 42CrMo side. The shapes of welding flashes are visibly different. The so-called "socks cylinder shape" flash forms in the IFW, but the so-called "butterfly wing shape" flash forms in CIFW. Compared to IFW, the length, diameter, and deformation of the whole welding joint in CIFW are found significant variations, which will affect the quality of welding joints.

3.2 XRD analysis of joint

XRD analysis results from the CIFW joint, shown in Fig. 3, indicate that the Fe–Ni intermetallic compounds and NbC intermetallic compounds are formed in the friction combining zone. The formation of intermetallic compounds can be attributed to elemental diffusion each other between dissimilar metals. This shows that the elemental diffusion does occur. The elemental diffusion is the dominant factor determining the success of the dissimilar welding joint formation, and the diffusion of Ti, Nb, Cr, Fe, and Ni from the base into the flashes improves the adhesion strength of the interface. This shows that the K418–42CrMo dissimilar metals form a strong metallurgical binding joint.

3.3 Elements diffusion

Figure 4 shows the micro-morphology and elemental diffusion in K418–42CrMo dissimilar metal IFW and CIFW joints, respectively. Based on the curve of the energy spectrum line scanning of main elements (Cr, Ni, and Fe element; other elements' diffusion is not considered), different feature zones can be identified marked. The conventional IFW joint can be

Table 3 The composition of quench-tempered alloy steel 42CrMo (wt%)

C	Cr	Mn	Mo	Si	S	P	Fe
0.38–0.45	0.90–1.20	0.50–0.80	0.15–0.25	0.20–0.406	≤0.040	≤0. 040	Balance

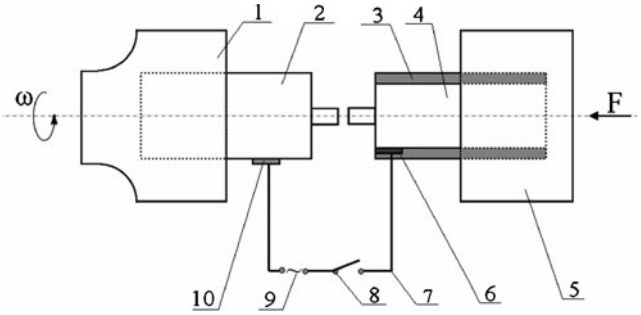

Fig. 1 The schematic for K418–42CrMo dissimilar metal in CIFW: *1* inertial flywheel, *2* K418 workpieces, *3* Insulating layer, *4* 42CrMo workpieces, *5* mobile fixture, *6* copper strip, *7* wire, *8* switch, *9* applied power source, and *10* carbon brush

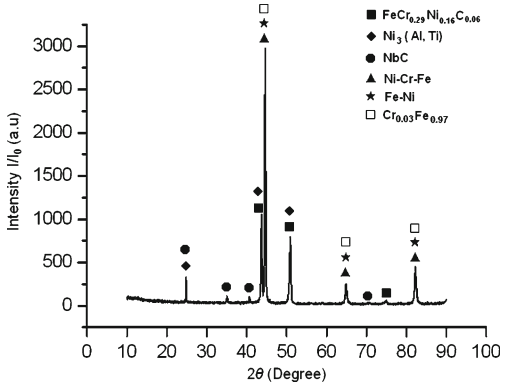

Fig. 3 The XRD diffraction patterns of K418–42CrMo dissimilar metal CIFW joint

divided into four different feature zones, i.e., zone 1–4 (see Fig. 4a). The CIFW joint can be divided into three different feature zones, i.e., zone 1′–3′ (see Fig. 4c).

The reference value is the relative intensity value 5 a.u. from the curve of the energy spectrum line scanning. It can be used to describe the diffusion behavior of these elements as a semiquantitative method. The element Ni or the element Cr is responsible for describing diffusion behavior on the K418 metal side. The element Fe is responsible for describing diffusion behavior on the 42CrMo metal side, based on the chemical composition of the base material.

Element diffusion with a lower relative intensity value (<5 a.u.) is ignored based on the energy spectrum line scanning. On the K418 side, the position with relative intensity value 5 a.u. of the element Fe is considered as the right boundary. Similarly, on the 42CrMo side, the position with relative intensity value 5 a.u. of an element Ni or Cr is considered as the left boundary. The feature zone and the boundaries are shown in Fig. 4.

In Fig. 4a and b, an element diffusion zone of 1 μm width (zone 2) appears on the 42CrMo side, based on the relative intensity value from 5 to 10 a.u. of the elements Ni or Cr on the curve of the energy spectrum line scanning. The elements Cr and Ni of the K418 base material are diffused in this zone. The interface friction bonding zone (zone 3) is gray and the width is about 1 μm, based on the clear boundary of the

Fig. 2 Macrostructure of K418–42CrMo dissimilar metal friction welding joints

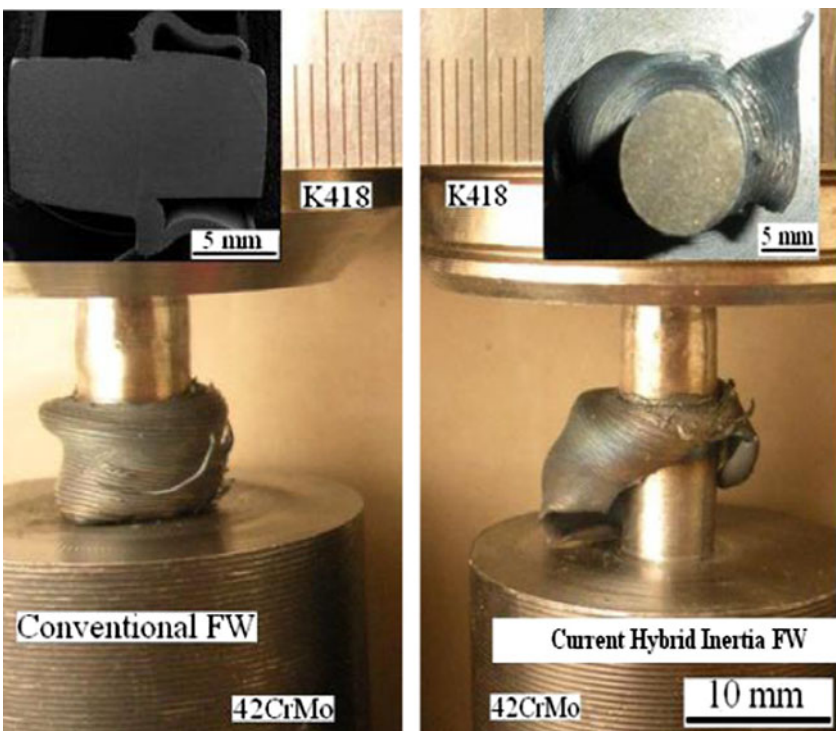

(a) IFW (b) CIFW

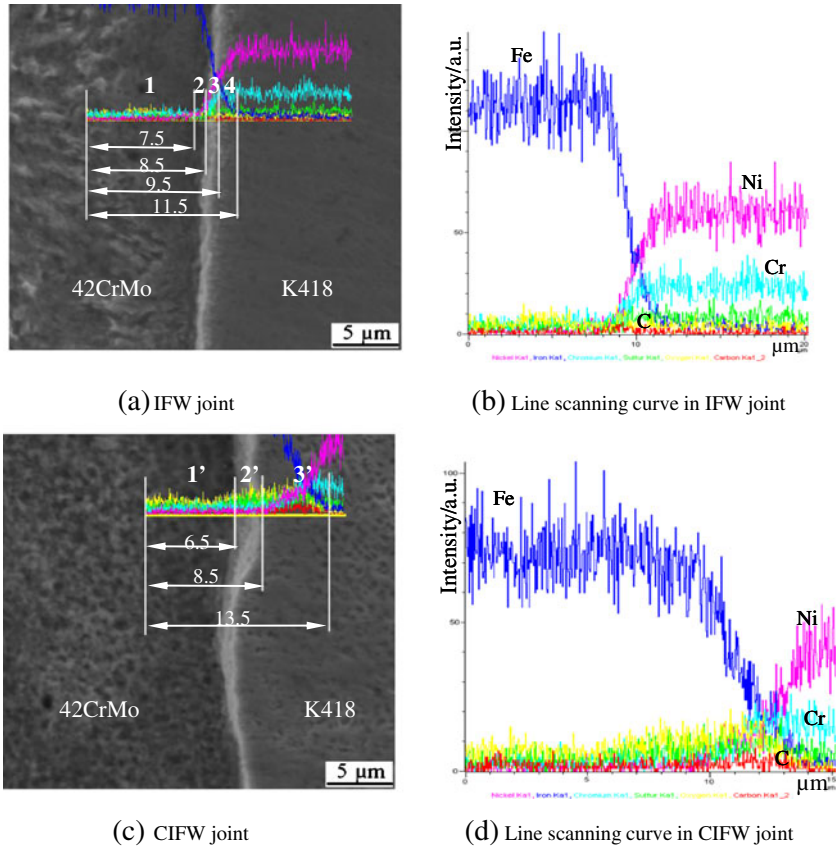

Fig. 4 Microstructure and element diffusion of K418–42CrMo dissimilar metal welding joint: *1* heat-affected zone of 42CrMo side, *2* elements diffusion zone of 42CrMo side, *3* interface friction bonding zone, *4* elements diffusion zone of K418 side, *1′* heat affected zone of 42CrMo side; *2′* interface friction bonding zone, and *3′* elements diffusion zone of K418 side

welding interface. Analyses of microstructure and energy spectrum show the interface friction bonding zone is made up of mixtures between K418 and 42CrMo base metals. The interface friction bonding zone does occur strong plastic deformation and dynamic recrystallization phenomenon. An element diffusion zone with 2 μm width is formed on the K418 side, and the transition behavior of the element Fe from the 42CrMo base metal appears on the K418 side. The carbon content changes little on the welding joint. Figure 4a also shows that the interface deformation in the IFW joint is a regular line.

In Fig. 4c, an elements diffusion zone of 3 μm width (zone 2′) appears on the 42CrMo side, based on the relative intensity value from 5 to 10 a.u. of elements Ni or Cr in the curve of the energy spectrum line scanning in Fig. 4d. The element Ni in the K418 base material is diffused into this zone. The gray interface friction bonding zone (zone 3′) is a wavy line with about 2 μm width, based on the clear boundary of the welding interface. The interface of the CIFW joint has a strong deformation and is an irregular line. The energy spectrum analysis shows that the interface friction bonding zone is formed mainly by K418. The width of the element diffusion zone (zone 4′) on the K418 side is 3 μm. The transition behavior of the element Fe from the 42CrMo base metal appears in the K418 side. The carbon content has little change in the whole of the welding joint.

3.4 Microhardness

Figure 5 shows the microhardness distribution of welding joints in IFW and CIFW. The friction bonding interface (welding seam line) is located at the origin position on the axial direction of the welding seam's cross-section.

According to the developing trend of the microhardness curve and the characteristics of the inertia friction welding joint, the K418–42CrMo dissimilar metal friction welding joint can be divided into three zones by the average microhardness values of K418 and 42 CrMo base materials (see in Fig. 5): hardened, softened, and base material zone. The softened zone (zone A and D) is caused by the relatively coarse grains, which formed in the HAZ near the welding seam line. Some researchers consider this to be the result of the overgrowth of local dynamic recrystallisation grains [25–28].

In hardened zone B, fine grains are produced by dynamic recrystallisation behavior, and element C diffusion is promoted from the 42CrMo base metal to the K418 side because the heat transfer and plastic deformation take place on the friction bonding interface. Strong carbide-forming elements, such as Nb, Ti, and Ni, on K418 side react with the element C from 42CrMo and form carbides that lead to hardening in this zone of the K418 side. The XRD analysis shows that NbC carbide is in the welding joint (shown in Fig. 3). On the other hand, the

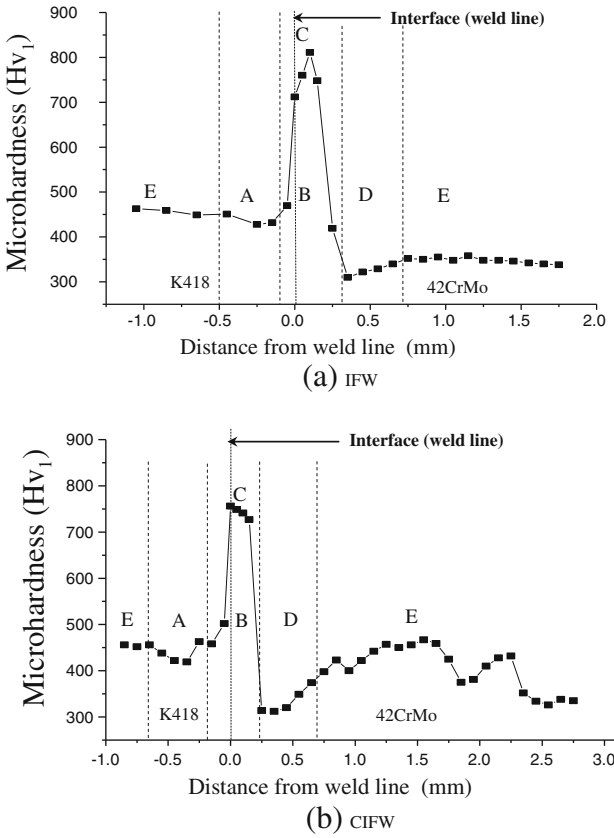

Fig. 5 Microhardness of K418–42CrMo dissimilar metal friction welding joint: **a** softened zone in K418 side, **b** hardened zone, **c** park value point, **d** softened zone in 42CrMo side, and **e** base material

width of hardened zone B in the K418 side of CIFW decreases, becoming smaller than that of IFW because of the heat treatment function from the additional current. However, the softened zone D in the 42CrMo side of CIFW is larger than that of IFW because the element diffusion region of the CIFW welding joint increases and extends as a result of the additional resistance heat.

The quenched martensite in zone B leads to the rapid increase of microhardness on the friction bonding interface. The peak microhardness value (point C) of conventional IFW joints (811 Hv, average value) is higher than that of CIFW joints at the same region (756 Hv, average value). This is related to the influence of element diffusion, especially the K418 base element diffusion toward the 42CrMo side across the interface in conventional IFW (shown in Fig. 4a, b). However, in CIFW, element diffusion only occurs in the K418 side (seen in Fig. 4c, d) of the welding joint. The solidification temperature gradient or continuous cooling transfer speed of the CIFW joint is smaller or slower than that of conventional IFW joints. In addition, the additional current leads to a large amount of resistance heat at the interface of CIFW joints; the considerable resistance heat has good heat treatment and preheat functions, which can improve the microstructure and decrease defects in the welding joint. Hence, the quenched martensite formation constituent in CIFW joints is more difficult to form than that in IFW joints, and the microhardness of CIFW joints has a little low park value in zone B.

In base material zone E (near HAZ), the average microhardness values of conventional IFW joints are 450 Hv on K418 side and 350 Hv on 42CrMo side; it is nearly the same as the average microhardness values of CIFW. However, the microhardness values of CIFW joints change more strongly than those of IFW joints.

The microhardness testing results show that the softened and hardened zones exist in both the 42CrMo side and K418 side of IFW joints. Compared to conventional IFW, the hybrid current can appreciably decrease the peak microhardness on the interface of the welding joint. The welding cracking tendency on the welding interface can be reduced because the intense variation of hardness of K418–42CrMo dissimilar metal welding joints will lead to heterogeneous strain, but the intense variation of hardness is held back by the hybrid current in CIFW.

3.5 Mechanical tensile strength

Because the center part has week bonding strength in the friction welding, and the workpieces are small in size, many microtensile test specimens (12 mm L × 3.9 mm W × 0.9 mm H) around the center part of the welding joint are prepared from IFW and CIFW joints. The maximum tensile force of the conventional IFW specimen is 1,361 N (average value); the tensile strength of IFW specimen is 388 MPa. The maximum tensile force of the CIFW specimen is 1,929 N (average value); the tensile strength of CIFW specimen is 549 MPa. It is clear that the tensile test result shows that the tensile strength of CIFW joints is better than that of IFW joints, as shown in Fig. 6.

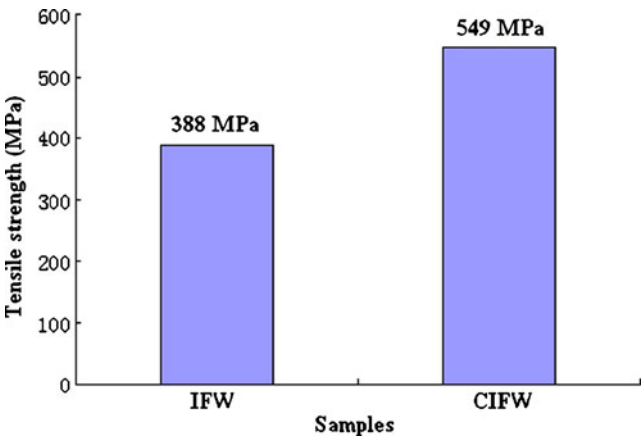

Fig. 6 Tensile strength results of K418–42CrMo dissimilar metal friction welding joint

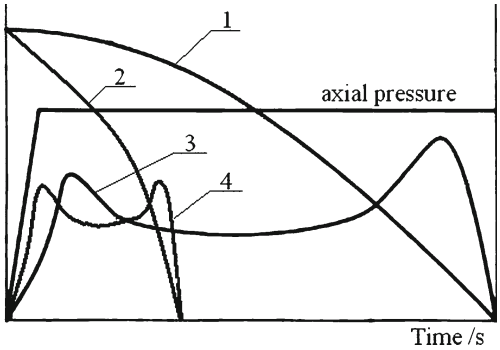

Fig. 7 Developing procedure of K418–42CrMo dissimilar metal in IFW and CIFW: *1* rotational speed of IFW, *2* rotational speed of CIFW, *3* torque of IFW, and *4* torque of CIFW

4 Discussion

4.1 Weld formation mechanism

The developing of K418–42CrMo dissimilar metal in conventional IFW and CIFW is illustrated in Fig. 7. As a result of the hybrid current, the welding time for CIFW is shorter than that for IFW. In conventional IFW, at the first stage of friction welding, only a few gibbous parts are in contact with one another on the initial rugged friction surface. The actual contact area is small. The adhesion and shear behaviors also occur on these primary contact points. Subsequently, these adhesion and shear behaviors significantly increase gradually as the friction area increases. For an ideal elastic–plastic material, the adhesive friction theory can be used to analyze this procedure or mechanism in friction welding.

The friction heat induces the plastic deformation zone to increase gradually in the boundary of the welding joint, and the welding flash forms because the high temperature viscosity metal layer is squeezed out. Some new contact parts are produced on the friction interface and begin to rub against each other again, until the original microrugged parts disappear partially or totally. Thus, the temperature distribution and heat transfer in the welding joint reach as a balance. The whole conventional IFW process lasts a long time with the time period being 3 s in the conditions of this experiment. During the friction stage, a viscosity metal layer on the contact surface is squeezed out and the small flash forms first. Then, at the beginning of the forge, many of the viscosity metal layers are squeezed out, such that a big flash finally forms. A so-called “socks cylinder shape” flash appears. The plastic deformation and temperature are enough to join two parts together, and the workpiece has an obvious axial length reduction after welding is finished.

In CIFW, at the beginning stage, only a few gibbous points have contact with one another; contact resistance is relatively large among the rugged interface. Because the main composition of K418 material is a Ni element, whose conductivity is stronger than that of the Fe element from 42CrMo metals, resistance heat is mainly produced in the 42CrMo side on the condition of the K418–42CrMo contact pair. Combined with the action of resistance heat and friction heat, the instantaneous considerably high temperature takes place on the friction surface, especially on the prime contact region. The metal deformation of these contact parts reaches the yield limit value of material rapidly. The state of contact pieces changes into the plastic deformation, resulting in the adhesion and occlusion on the interface of the contact surface. These adhesion points are also torn and joined repeatedly by the relative rotation and extrusion action in the friction welding process.

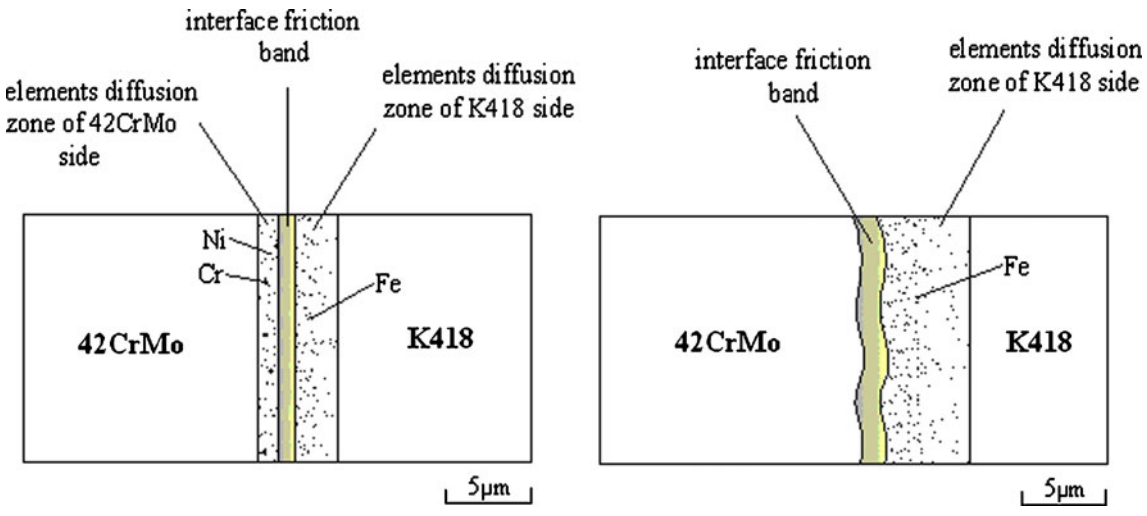

Fig. 8 The schematic for interface features in K418–42CrMo dissimilar metal friction welding joint

With the workpiece contact increase in the friction welding process, large amounts of resistance heat and friction heat are generated, and the metal plastic deformation level increases rapidly. In some periods, the temperature distribution and heat transfer on the welding joint will reach a balance. Because the resistance heat is generated by the hybrid current, the whole thermal flux of CIFW joints includes both resistance heat and friction heat. Besides thermal flux, the flash formation depends on both mechanical properties and thermophysical properties of the materials. The K418 possesses good creep strength, thermal fatigue properties, and oxidation resistance. Its high temperature strength is significantly higher than that of 42CrMo. In the condition of CIFW, extra resistance heat is produced on the 42CrMo side. In a short welding period, the high-temperature viscosity metal in the 42CrMo side is squeezed out and thrown off from the rotation spindle. Because the high-temperature viscosity metal deformation layer is not thick, a so-called "butterfly wing shape" flash is formed under the effect of friction and forge forces (shown in Fig. 2).

Due to large amounts of resistance heat generation in CIFW, a large elastic–plastic stress contact area can be rapidly translated to the plastic deformation layer. The flowing of viscosity metal is enhanced under the influence of the shear stress, so the actual contact area is getting bigger in a short time. Because the viscosity deformation layers are squeezed out quickly, the friction coefficient increases significantly on the left rough surface. Then, many occlusion points on the contact surface induce the contact resistance to increase significantly again, and there is a strong plastic deformation because the instantaneous high temperature is produced repeatedly. Therefore, at the same technical conditions, the welding duration time for CIFW is shorter than that in conventional IFW, and the axial length of the welding joint also changes a little.

4.2 Interfacial features

In the comparison between conventional IFW and CIFW, shown in Fig. 5a and c, the interface microconstituent pattern of K418–42CrMo dissimilar metal joints is illustrated in Fig. 8.

The interface deformation of IFW joints is smaller than that of CIFW. The interfacial line between K418 and 42CrMo of IFW joints is a straight line, but the interfacial line of CIFW joints demonstrates a wavy and rugged interlocking pattern. The wavy and rugged interfacial structure characteristic is of the mechanical interlocking function, which promotes bonding and interlocking between K418 and 42CrMo dissimilar metals. The friction welding interfacial tensile strength of CIFW joints appeared to increase owing to the jagged, interlocking interfacial structure (see in Fig. 6).

At the same time, there is a great difference in the curve of the energy spectrum line scanning between the IFW and CIFW joints. The curves of the energy spectrum line scanning of a main element (such as Cr, Ni, and Fe) on CIFW joints are of gentle gradient change characteristic, which are more faired and continuous than those in IFW joints. The width of every feature zone in CIFW joints is larger than that in IFW. It is the hybrid current that makes the resistance heat production considerable; the resistance heat and friction heat flow into the friction welding joint, so the strong plastic deformation and element diffusion have occurred in the friction contact region of the joint, although the welding time is short in friction welding. Because the high temperature strength and electrical conductivity of the 42CrMo material are less than those of the K418 material, it is obvious that the 42CrMo side of CIFW joints can result in a large resistance heat production and plastic deformation. On the other hand, owing to the heat treatment function of resistance heat from the hybrid current loading, the diffusion behaviors of main elements can be enhanced in CIFW joints. Hence, the curve of the energy spectrum line scanning of major elements is more flat in CIFW joints, the diffusion distance of CIFW is longer than that of IFW joint, and the scatter degree is stronger than that of IFW joint. The whole element diffusion zone of CIFW joints migrates from the 42CrMo side to the K418 side (see in Fig. 8b). The width of the element diffusion zone increases in CIFW joints. The alternating diffusion bonding interfacial structure is formed in K418 and 42CrMo dissimilar metal joints.

Theoretically, the strong plastic deformation and element diffusion help improve the quality of friction welding [32–34]. The hybrid current thus makes the resistance heat to help produce a stronger joint and provide an effective method for dissimilar metal joining or welding. The mixed interfacial structures in CIFW are of the partial occlusion, mechanical interlocking, and diffusion bonding characteristics, which all help increase the strength of K418–42CrMo dissimilar metal friction welding joint.

5 Conclusions

1. The hybrid current has a significant influence on interfacial characteristics of IFW joints. Due to the combined action from resistance heat and friction heat, the required welding time for CIFW to complete a qualified welding joint is shortened. The soften deformation is also reduced.
2. The friction bonding interface of the CIFW joint changed into a wavy and rugged mechanical interlocking structure, and the flash pattern of the joints has changed from the "Socks cylinder shape" flash of IFW joints into the "butterfly wing shape" flash of CIFW joints.
3. Compared to that in the conventional IFW joint, the width of the elements diffusion zone in CIFW joints increases.

The microhardness on the bonding interface is decreased appreciably, which can be attributed to the heat treatment from the resistance heat.

4. The tensile strength of CIFW joints is better than that of IFW joints because the mixed interfacial structures of CIFW are of the partial occlusion, mechanical interlocking, and diffusion bonding characteristics, which benefit the strength of K418–42CrMo dissimilar metal friction welding joints.

Acknowledgments The authors gratefully acknowledge the support from the Natural Science Foundation of China (no. 51075413), the Fundamental Research Funds for the State Key Lab of Mechanical Transmission (SKLMT-ZZKT-2012MS08), Excellent Talents Project in Universities of Chongqing Municipal Education Commission (2010), Sharing Fund of Chongqing University's Large-scale Equipment, the Fundamental Research Funds for the Central University (CDJRC11280002/CDJZR13280006), and the State Key Lab of Mechanical Transmission Chongqing University, China. The authors would like to thank Prof. Dr. Zhang YM, Ms. Amber Short at the University of Kentucky in the USA for helpful discussion.

References

1. Kalsi NS, Sharma VS (2011) A statistical analysis of rotary friction welding of steel with varying carbon in workpieces. Int J Adv Manuf Technol 57:957–967
2. Reddy GM, Rao KS (2009) Microstructure and mechanical properties of similar and dissimilar stainless steel electron beam and friction welds. Int J Adv Manuf Technol 45:875–888
3. Sathiya P, Aravindan S, Haq AN (2007) Effect of friction welding parameters on mechanical and metallurgical properties of ferritic stainless steel. Int J Adv Manuf Technol 31:1076–1082
4. Meshram SD, Mohandas T, Reddy G (2007) Friction welding of dissimilar pure metals. J Mater Process Technol 184:330–337
5. Huang ZW, Li HY, Preuss M, Karadge M, Bowen P, Bray S, Baxter G (2007) Inertia friction welding dissimilar nickel-based superalloys alloy 720Li to IN718. Metall Mater Trans A 38:1608–1620
6. Sare C, Ismail E (2009) Investigation of the mechanical properties and microstructure of friction welded joints between AISI 4140 and AISI 1050 steels. Mater Des 30:970–976
7. Moat RJ, Hughes DJ, Steuwer A, Iqbal N, Preuss M, Bray SE, Rawson M (2009) Residual stresses in inertia-friction-welded dissimilar high-strength steels. Metall Mater Trans A 40:2098–2108
8. Luo J, Zhao GJ, Luo Q, Wang XJ, Xu XL (2010) Element diffusion on interface of 35CrMnSi/T3 inertial radial friction weld. J Xi'an Jiaotong Univ 44:63–67
9. Sahin M (2009) Joining of stainless steel and copper materials with friction welding. Ind Lubr Tribol 61:319–324
10. Kimura M, Kasuya K, Kusaka M, Kaizu K, Fuji A (2009) Effect of friction welding condition on joining phenomena and joint strength of friction welded joint between brass and low carbon steel. Sci Technol Weld Join 14:404–412
11. Shin HS, Park JS, Jung YC, Ahn JH, Yokoyama Y, Inoue A (2009) Similar and dissimilar friction welding of Zr–Cu–Al bulk glassy alloys. J Alloys Compd 483:182–185
12. Wang D, Xiao BL, Ma ZY, Zhang HF (2009) Friction stir welding of Zr55Cu30Al10Ni5 bulk metallic glass to Al-Zn-Mg-Cu alloy. Scr Mater 60:112–115
13. Shoji T, Kawamura Y, Ohno Y (2004) Friction welding of bulk metallic glasses to different ones. Metall Mater Trans A 375–377: 394–398
14. Sahin M (2009) Joining of stainless-steel and aluminium materials by friction welding. Int J Adv Manuf Technol 41:487–497
15. Shinoda T, Miyahara K, Ogawa M, Endo S (2001) Friction welding of aluminum and plain low carbon steel. Weld Int 15:438–445
16. Seli H, Ismail A, Rachman E, Ahmad ZA (2010) Mechanical evaluation and thermal modelling of friction welding of mild steel and aluminium. J Mater Process Technol 210:1209–1216
17. Taban E, Gould JE, Lippold JC (2010) Dissimilar friction welding of 6061-T6 aluminum and AISI 1018 steel: Properties and microstructural characterization. Mater Des 31:2305–2311
18. Zimmerman J, Wlosinski W, Lindemann ZR (2009) 2Thermo-mechanical and diffusion modelling in the process of ceramic–metal friction welding. J Mater Process Technol 9:1644–1653
19. Dey HC, Ashfaq M, Bhaduri AK, Rao KP (2009) Joining of titanium to 304L stainless steel by friction welding. J Mater Process Technol 209:5862–5870
20. Fukumoto S, Inoue T, Mizuno S, Okita K, Tomita T, Yamamoto A (2010) Friction welding of TiNi alloy to stainless steel using Ni interlayer. Sci Technol Weld Join 15:124–130
21. Wang Y, Luo J, Wang XM, Xu XL (2013) Interfacial characterization of T3 copper/35CrMnSi steel dissimilar metal joints by inertia radial friction welding. Int J Adv Manuf Technol 68: 1479–1490
22. Nada R, Aleksandar S, Milorad J, Vukic L, Ruzica N, Bozidar K (2009) Quality analysis of Al–Cu joint realized by friction welding. Tehnicki Vjesnik 16:3–7
23. Sathiya P, Aravindan S, Haq AN (2005) Mechanical and metallurgical properties of friction welded AISI 304 austenitic stainless steel. Int J Adv Manuf Technol 26:505–511
24. Chen DJ, Xu XL, Xu YZ, Wu W (2004) Quality controlling method of K418 and 42CrMo inertia friction welding joints. Weld Join 2:46–48
25. Lee JW (1992) Inertia friction welding of a gas turbine rotor. Weld Rev Int 11:189–192
26. Du SG, Fu L, Wang JW, Cao Y (2003) Forming mechanism of carbide band in friction welding joint of superalloy K418 and steel 42CrMo. Chinese J Nonferr Metal 13:323–327
27. Du SG, Fu L, Cao Y, Wang JW (2004) On strengthening the friction welding joint between K418 turbo disk and 42CrMo shaft. J Northwest Polytech Univ 22:112–115
28. Chen DJ, Xu XL, Xu YZ, Wu W (2008) Inertia friction welding of dissimilar materials between K418 turbine disk and 42CrMo shaft. Weld Join 6:58–60, 68
29. Luo J, Wang XJ, Wang JX (2009) New technological methods and designs of stir head in resistance friction stir welding. Sci Technol Weld Join 14:650–654
30. Fu L, Du SG (2006) Effects of external electric field on microstructure and property of friction welded joint between copper and stainless steel. J Mater Sci 41:4137–4142
31. Wang SY, Zhang GF, Qiu FX, Guo Y (1994) Heat soerce behavior of conducting friction welding and its influence on technology process. J Xi'an Jiaotong Univ 28:130–134
32. Teker T (2013) Evaluation of the metallurgical and mechanical properties of friction-welded joints of dissimilar metal combinations AISI2205/Cu. Int J Adv Manuf Technol 66:303–310
33. Arivazhagan N, Singh S, Prakash S, Reddy GM (2008) An assessment of hardness, impact strength, and hot corrosion behaviour of friction-welded dissimilar weldments between AISI 4140 and AISI 304. Int J Adv Manuf Technol 39:679–689
34. Sunay TY, Sahin M, Altintas S (2009) The effects of casting and forging processes on joint properties in friction-welded AISI 1050 and AISI 304 steels. Int J Adv Manuf Technol 44:68–79